

## **Chapter 3**

# **EFFECT OF PLAN AND HEIGHT ASPECT RATIOS ON ALONG WIND AND ACROSS WIND LOADS ON SUPER HIGH RISE BUILDINGS**

### **3.1 Introduction**

The correct estimation of Equivalent Static Wind Load (ESWL), particularly the across wind loading on super high-rise buildings, holds paramount significance and is currently an active area of research. In this study, A MATLAB program has been developed, facilitating a parametric study based on the formulation proposed by Quan and Gu (2012). The study aims to assess the across wind ESWL for buildings with a height of 300 meters. The investigation considers a range of plan aspect ratios from 0.5 to 2. Moreover, the study also explores the effect of varying height aspect ratios ranging between 4 and 9. Overall, the MATLAB program is a valuable tool for conducting this research, enabling a comprehensive evaluation of wind ESWL across super-tall structures. The results obtained from this parametric study will contribute significantly to advancing our understanding of wind loads on super high-rise buildings. A summary of this chapter is as follows: This chapter delves into the calculation of along wind load as per the IS 875 (Part 3): 2015 guidelines. It then comprehensively discusses the Quan and Gu (2012) analytical method for calculating the across wind ESWL. It then outlines the step-by-step procedure to calculate the across wind ESWL. The chapter then moves on to describe the methodology adopted in the study. It covers all the parameters involved in calculating across wind ESWL in the Input data sections.

Additionally, it highlights the specific plan and height aspect ratio chosen for this study. Next, the chapter presents the results of the study, discussing the findings and outcomes in detail. Finally, it concludes with closing remarks summarizing the key takeaways from the entire investigation.

### **3.2 Indian standard procedure to calculate Along wind load**

For assessing the dynamic along-wind and across-wind loads on tall structures, most of the international standards utilize the gust factor method initially formulated by Davenport (1967). Along wind load in the present study is calculated using the Indian code [IS 875 (Part 3): 2015]. It uses hourly mean wind speed which incorporates the terrain category factor, probability factor, topography factor, and importance factor for the cyclonic region. Design hourly mean wind pressure conforming to hourly wind speed is obtained by the square of hourly wind speed multiplied by a constant of 0.6. Indian standard embraced the gust factor approach for the calculation of along wind loads and responses. Gust factor incorporates the mean component, background component, and resonant component of wind load.

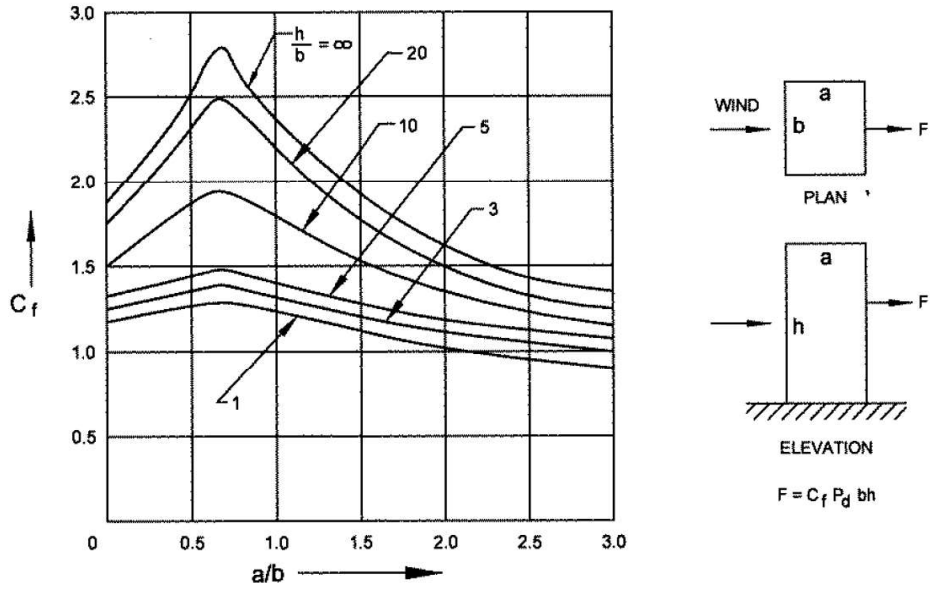
The design peak along wind base bending moment ( $M_a$ ) has been calculated by integrating the moments resulting from design peak values acting at different heights,  $z$  along the height of building expressed in Equation (3.1).  $F_z$  is the design peak ESWL on the building at any height  $z$  considering along wind load.

$$M_a = \sum F_z Z \quad (3.1)$$

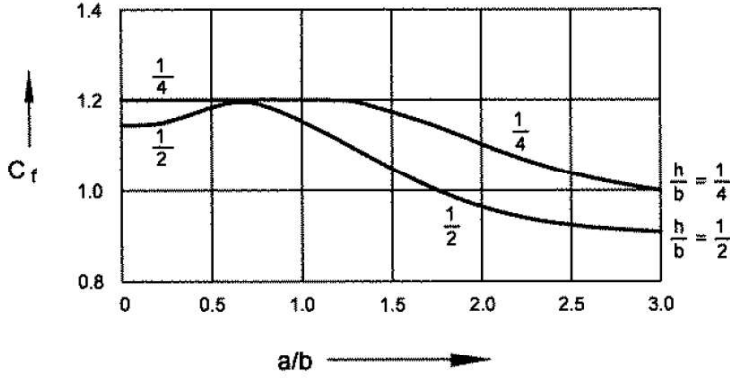
Considering along wind loading, the design peak ESWL on the building is obtained from Equation (3.2).

$$F_z = C_{f,z} A_z \bar{p}_d G \quad (3.2)$$

where,  $A_z$  is the effective frontal area ( $m^2$ ) of the building at any height  $z$ , the design hourly mean wind pressure ( $\bar{p}_d$ ) corresponding to the design hourly mean wind speed ( $\bar{V}_{z,d}$ ) at height  $z$  and obtained as  $0.6\bar{V}_{z,d}^2$ .  $\bar{V}_{z,d}$  is the design hourly mean wind speed at height  $z$  and can be calculated from the clause 6.4 of IS 875 (Part 3): 2015.  $C_{f,z}$  is the drag force coefficient of the building corresponding to the area  $A_z$  and is seen from Figure 3.1 (which is figure 4 of IS 875 (Part 3): 2015).



(a) Values of  $C_f$  versus  $a/b$  for  $h/b \geq 1$



(b) Values of  $C_f$  versus  $a/b$  for  $h/b < 1$

**Figure 3.1** Force coefficient for rectangular clad buildings in uniform flow (Figure 4 of IS 875 (Part 3): 2015)

G is the gust factor and is calculated from Equation (3.3).

$$G=1+r \sqrt{\left[ g_v^2 B_s (1 + \phi)^2 + \frac{H_s g_R^2 S E}{\beta} \right]} \quad (3.3)$$

Where, r = roughness factor which is twice of turbulence intensity,  $g_v$  = peak factor for upwind velocity fluctuations which is considered as 4.0 for this case,  $B_s$  = background factor which is calculated as Equation (3.4).

$$B_s = \frac{1}{\left[ 1 + \frac{\sqrt{0.26(h-s)^2 + 0.46b_{sh}^2}}{L_h} \right]} \quad (3.4)$$

$b_{sh}$  is the average breadth of the building/structure between height s and h,  $L_h$  is the measure of effective turbulence length scale at the height, h in meter. For terrain category 4,  $L_h$  is calculated as  $70\left(\frac{h}{10}\right)^{0.25}$ .  $\phi$  = factor to account for second order turbulence intensity and can be calculated from Equation (3.5).

$$\phi = \frac{g_v I_{h,i} \sqrt{B_s}}{2} \quad (3.5)$$

$I_{h,i}$  = turbulence intensity at height h in terrain category i. S = Size reduction factor and can be calculated from Equation (3.6).

$$S = \frac{1}{\left[ 1 + \frac{3.5 f_a h}{\bar{V}_{h,d}} \right] \left[ 1 + \frac{4 f_a b_{0h}}{\bar{V}_{h,d}} \right]} \quad (3.6)$$

Where,  $b_{0h}$  is the average breadth of the building/structure between 0 and h.

$g_R$  = peak factor for resonant response ( $\sqrt{[2 \ln(3600 f_a)]}$ ),  $H_s$  = height factor for resonance response  $\left(1 + \left(\frac{s}{h}\right)^2\right)$

$E$  = spectrum of turbulence in the approaching wind stream which can be calculated from Equation (3.7).

$$E = \frac{\pi N}{(1 + 70.8N^2)^{5/6}} \quad (3.7)$$

Where,  $N$  is effective reduced frequency  $\left(\frac{f_a L h}{\bar{V}_{h,d}}\right)$ ,  $f_a$  is the first mode natural frequency of the building/structure in along wind direction, in Hz,  $\bar{V}_{h,d}$  is the design hourly mean wind speed at height,  $h$  in m/s,  $\beta$  = damping coefficient of building taken as 0.020 for RCC structures. All the parameters used above are taken appropriately as per the IS 875(Part 3): 2015.

### 3.3 Across wind ESWL

Across wind load in this study is estimated using the formulation given by Quan and Gu (2012). The results from the formulation of Quan and Gu (2012) compare well with AIJ recommendations. Quan and Gu (2012) proposed a mathematical model to evaluate across wind ESWL on super high rise buildings based on the studies done by Liang *et al.* (2002) and Cheng *et al.* (2001). It is important to note that the across wind equivalent static wind loads is calculated individually as resonant and background component. The inertial force principle is used for the computation of the resonant component in which the effect of aerodynamic damping is considered. Based on the background moment responses at various heights, the background component is stated as a cubic equation depending on height and calculated using base moment coefficients. The assumptions of the analytical method is stated first after that the detailed procedure to evaluate the across wind ESWL is described.

### 3.3.1 Assumptions of Quan and Gu (2012) formulation

(1) Super high-rise buildings with uniform rectangular cross-sections have negligible mean across-wind loads due to shape symmetry, that is

$$\bar{p}(z) = 0 \quad (3.8)$$

(2) High modes exhibit negligible resonant responses in comparison with the first mode, and the first mode shape can be described as

$$\varphi_1(z) = (z/H)^\beta \quad (3.9)$$

Where  $\beta$  is the mode shape index.

(3) The sections of the super high-rise buildings are symmetric rectangular and the across-wind loads are considered for an approaching wind parallel to body axis of target building.

(4) The target super high-rise buildings have plan aspect ratios of less than 2.0 and aspect ratios between 4 to 9.

### 3.3.2 Resonant component

Equation (3.10) represents the wind-induced response of a high-rise building

$$y^{(r)}(z, t) = \sum_{i=1}^{\infty} Y_i^{*(r)}(t) \varphi_i(z) \quad (3.10)$$

Where,  $\varphi_i(z)(i=1,2,\dots)$  is the  $i^{\text{th}}$  mode shape of the building,  $y^{(r)}(z, t)$  is the  $r^{\text{th}}$  derivative of the displacement response of the structure at height  $z$  and time  $t$ , and  $Y_i^{*(r)}$  is the  $r^{\text{th}}$  derivative of the generalized displacement of the  $i^{\text{th}}$  mode. Therefore, to obtain the generalized displacement,  $Y_i^*(t)$ , can be obtained from Equation 3.11.

$$\ddot{Y}_i^* + 2(\zeta_{si} + \zeta_{ai})\omega_i \dot{Y}_i^* + \omega_i^2 Y_i^* = F_i^*(t)/M_i^* \quad (3.11)$$

Where,  $F_i^*(t) = \int_0^H w(z, t) \varphi_i(z) dz$  is the  $i^{th}$  generalized wind force and  $\zeta_{si}$  and  $\zeta_{ai}$  are the structural and aerodynamic damping ratios, respectively; and The  $M_i^*$  is the  $i^{th}$  generalized mass expressed in Equation (3.12), where  $m(z)$  is the mass per unit height at height  $z$ .

$$M_i^* = \int_0^H m(z) \times \varphi_i^2(z) dz \quad (3.12)$$

The power spectral density solution of  $Y_i^{*(r)}$  can be derived in terms of random vibration theory and can be expressed in Equation (3.13).

$$S_{Y_i^{*(r)}}(f) = \frac{(2\pi f)^{2r} |H_i(f)|^2 S_{F_i^*}(f)}{(2\pi f_i)^4 M_i^{*2}} \quad (3.13)$$

Where  $S_{F_i^*}(f)$  is the  $i^{th}$  generalized aerodynamic force power spectral density. According to the principle of high-frequency balance technique,  $S_{F_i^*}(f)$  can be computed based on the corrected base moment power spectral density of the building.  $|H_i(f)|^2$  is the transfer function of the building given in Equation (3.14)

$$|H_i(f)|^2 = \frac{1}{(1 - (f/f_i)^2)^2 + 4(\zeta_{si} + \zeta_{ai})^2 (f/f_i)^2} \quad (3.14)$$

From Equation (3.13), the spectral density of the generalized displacement power is shown in Equation (3.15).

$$S_{Y_i^*}(f) = \frac{|H_i(f)|^2 S_{F_i^*}(f)}{(2\pi f_i)^4 M_i^{*2}} \quad (3.15)$$

The standard deviation of the generalized displacement can be written as Equation (3.16).

$$\sigma_{Y_i^*}^2 = \int_0^\infty S_{Y_i^*}(z, f) df = \int_0^\infty \frac{|H_i(f)|^2 S_{F_i^*}(f)}{(2\pi f_i)^4 M_i^{*2}} df \quad (3.16)$$

Equation (3.16) can be approximately divided into two parts, background part and resonant part and can be simplify as Equation (3.17).

$$\sigma_{y_i^*}^2 \approx \frac{1}{(2\pi f_i)^4 M_i^{*2}} \left( \int_0^{f_i} S_{F_i^*}(f) df + \frac{\pi f_i S_{F_i^*}(f_i)}{4(\zeta_{si} + \zeta_{ai})} \right) \quad (3.17)$$

From Equation (3.10-3.17), the displacement standard deviation at height  $z$  can be computed using the Equation (3.18-3.20).

$$\sigma_{y(z)}^2 = \sigma_{yR(z)}^2 + \sigma_{yB(z)}^2 \quad (3.18)$$

$$\sigma_{yR(z)}^2 \approx \sum_{i=1}^n \frac{\varphi_i^2(z)}{(2\pi f_i)^4 M_i^{*2}} \cdot \frac{\pi f_i S_{F_i^*}(f_i)}{4(\zeta_{si} + \zeta_{ai})} \quad (3.19)$$

$$\sigma_{yB(z)}^2 = \sum_{i=1}^n \frac{\varphi_i^2(z) \cdot \int_0^{f_i} S_{F_i^*}(f) df}{(2\pi f_i)^4 M_i^{*2}} \quad (3.20)$$

Where  $\sigma_{yR(z)}$  and  $\sigma_{yB(z)}$  are the resonant and background components of RMS displacement, respectively.

Based on the assumptions of Quan and Gu (2012) the resonant component of the RMS displacement response can be approximately derived from Equation (3.19) as Equation (3.21).

$$\sigma_{yR(z)}^2 = \frac{(z/H)^{2\beta}}{(2\pi f_1)^4 M_1^{*2}} \cdot \frac{\pi f_1 S_{F_1^*}(f_1)}{4(\zeta_{s1} + \zeta_{a1})} \quad (3.21)$$

The peak resonant ESWL refers to the inertial force acting on the building, as explained by Zhou *et al.* (1999a) is expressed in Equation (3.22).

$$\hat{p}_R(z) = g_R m(z) \omega_1^2 \sigma_{yR1(z)} = g_R \cdot \frac{m(z)(z/H)^\beta}{M_1^*} \sqrt{\frac{\pi f_1 S_{F_1^*}(f_1)}{4(\zeta_{s1} + \zeta_{a1})}} \quad (3.22)$$

Where,  $g_R$  is the peak factor of the resonant response, illustrated in Equation (3.23), and proposed by Davenport (1967).  $S_{F_1^*}(f_1)$  is the base moment power spectral density of the building model and can be obtained from wind tunnel test in the case of linear first mode *i.e.*  $\beta = 1$ . Many prominent researchers have analysed the across-wind base moment power spectral density of tall buildings with the help of wind tunnel testing.[Gu and Quan

(2004), Katagiri *et al.* (1995), Liang *et al.* (2002) Nishimura *et al.* (1999) and Yeh *et al.* (1997)]

$$g_R \approx \sqrt{2\ln(600f_l)} + \frac{0.5772}{\sqrt{2\ln(600f_l)}} \quad (3.23)$$

In Equation (3.23)  $f_l$  is the fundamental frequency of the structure. Based on series of wind tunnel tests Gu and Quan (2004) proposed the analytical formula (Equation 3.24 and 3.25) of across-wind base moment power spectral density for rectangular high-rise buildings with aspect ratios 4 to 9 and plan aspect ratio ( $\alpha_{db}$ ) 0.5 to 2.

$$f_1 S_{F_1^*}(f_1) = \Phi S_M^*(n) \{w_H B H\}^2 \quad (3.24)$$

$$S_M^*(n) = \frac{S_p \eta (n/f_p)^\lambda}{\{1 - (n/f_p)^2\}^2 + \eta (n/f_p)^2} \quad (3.25)$$

where,  $\Phi$  is the correction factor in this study it is considered as unity,  $w_H$  is the approaching wind pressure at the height of target building ( $0.5\rho U_H^2$ ),  $S_p$  is the amplitude parameter,  $f_p$  is the location parameter,  $\eta$  is the band width parameter,  $\lambda$  is the deflection parameter and  $\alpha_{hr}$  is the height ratio,  $\alpha_w$  is a parameter based upon turbulence intensity ( $I_H$ ) at height of the target building,  $n=f B/U_H$  is the reduced frequency,  $f$  is the frequency of the structure. These factors are calculated using Equations (3.26) to (3.32).

$$S_p = (0.1\alpha_w^{0.4} - 0.0004e^{\alpha_w}) \times (0.84\alpha_{hr} - 2.12 - 0.05\alpha_{hr}^2) \times (0.422 + \alpha_{db}^{-1} - 0.08\alpha_{db}^{-2}) \quad (3.26)$$

$$f_p = 10^{-5} (191 - 9.48\alpha_w + 1.28\alpha_{hr} + \alpha_{hr}\alpha_w) \times (68 - 21\alpha_{db} + 3\alpha_{db}^2) \quad (3.27)$$

$$\eta = (1 + 0.00473e^{1.7\alpha_w}) \times (0.065 + e^{1.26 - 0.63\alpha_{hr}}) e^{1.7 - 3.44/\alpha_{db}} \quad (3.28)$$

$$\lambda = (-0.8 + 0.06\alpha_w + 0.0007e^{\alpha_w}) \times (-\alpha_{hr}^{0.34} + 0.00006e^{\alpha_{hr}}) \times (0.414\alpha_{db} + 1.67\alpha_{db}^{-1.23}) \quad (3.29)$$

$$\alpha_{hr} = H/\sqrt{BD} \quad (3.30)$$

$$\alpha_{db} = D/B \quad (3.31)$$

$$\alpha_w = 4.2 - 4e^{3.7 - 60I_H} \quad (3.32)$$

The first mode aerodynamic damping ratio( $\zeta_{a1}$ ) is calculated from the Quan *et al.* (2005) as represented in Equation (3.33). where  $U^*$  is reduced wind velocity and calculated as  $U^* = U_H/f_1B$ .

$$\zeta_a = \frac{0.0025 \left(1 - (U^*/9.8)^2\right) (U^*/9.8) + 0.000125 (U^*/9.8)^2}{(1 - (U^*/9.8)^2)^2 + 0.0291 (U^*/9.8)^2} \quad (3.33)$$

After substituting Equation (3.24) into Equation (3.22) leads to Equation (3.34).

$$\hat{p}_R(z) = \frac{Hm(z)}{M_i^*} B_{WH} \left(\frac{z}{H}\right)^\beta g_R \sqrt{\frac{\pi \Phi S_M^*(f_1)}{4(\zeta_{s1} + \zeta_{a1})}} \quad (3.34)$$

### 3.3.3 Background component

Background response refers to a quasi-static reaction resulting from variations in turbulent wind, characterized by frequencies insufficient to trigger any resonant behaviour (Holmes 2001). It is essential to note that the structural dynamics do not influence the background segment of the equivalent static wind load or the dynamic reaction of buildings. The background component of across-wind loads is determined by considering the vertical distribution of background moment responses at various heights. This distribution is then represented as a cubic equation of relative height. The computation involves utilizing base moment coefficients to quantify the background effects accurately.

In this current study, wind pressure data obtained from wind tunnel tests conducted by Tang (2006) on a building model with a square-section and an aspect ratio of 6 in both open country and urban terrain are utilized. These data serve as the basis for calculating the Root Mean Square (RMS) background wind load as part of the research process. The peak back ground ESWL as suggested by Quan and Gu (2012) can be written as Equation (3.35).

$$\hat{p}_B(z) = (0.65 + 1.3z + 7z^2 - 7.5z^3)g_B C_{M-B0} B w_H \quad (3.35)$$

Where,  $g_B$  is the peak factor for the background component and is taken as 3.5 in this study and it generally ranges between 2.5 to 5.  $C_{M-B0}$  is the background base moment coefficient as shown in Equation (3.36) proposed by Quan *et al.*(2012).

$$C_{M-B0} = 0.182 - 0.019\alpha_{db}^{-2.54} + 0.054\alpha_w^{-0.91} \quad (3.36)$$

### 3.3.4 Peak across wind ESWL

The peak ESWL combined with background and resonant component can be written as Equation (3.37).

$$\hat{p}(z) = \sqrt{\hat{p}_R(z)^2 + \hat{p}_B(z)^2} \quad (3.37)$$

Where  $\hat{p}_B(h)$  and  $\hat{p}_R(z)$  can be calculated using Equation (3.34 and 3.35).

### 3.3.5 Across-wind acceleration

The generalized acceleration power spectral density of the first mode can be obtained from Equation (3.13) and written as Equation (3.38).

$$S_{\ddot{y}_i^{*(r)}}(f) = \frac{f^4 |H_1(f)|^2 S_{F_1^*}(f)}{f_1^4 M_1^{*2}} \quad (3.38)$$

Based on the Assumption (2) of article (3.3.1), the RMS acceleration response at height  $z$  is shown as Equation (3.39).

$$\sigma_a^2(z) = \int_0^\infty S_y(z, f) df = \varphi_1^2(z) \cdot \int_0^\infty S_{\ddot{y}_1^*}(f) df \quad (3.39)$$

Substituting Equation (3.14) into Equation (3.38) and then putting it into Equation (3.39), so Equation (3.39) can be rewritten as Equation (3.40).

$$\sigma_a^2(z) = \frac{\varphi_1^2(z)}{f_1^4 M_1^{*2}} \int_0^\infty \frac{f^4 S_{F_1^*}(f)}{(1 - (f/f_1)^2)^2 + 4(\zeta_{s1} + \zeta_{a1})^2 (f/f_1)^2} df \quad (3.40)$$

The above Equation (3.40) can be rewritten with approximation as Equation (3.41).

$$\sigma_a^2(z) = \frac{\varphi_1^2(z)}{M_1^{*2}} \int_0^{f_1} S_{F_1^*}(f) (f/f_1)^4 df + \frac{\varphi_1^2(z)}{M_1^{*2}} \cdot \frac{\pi f_1 S_{F_1^*}(f_1)}{4(\zeta_{s1} + \zeta_{a1})} \quad (3.41)$$

The first term of the above equation is negligible due to quartic ratio of frequency.

Therefore, the RMS acceleration response at height z can be calculated roughly as

Equation (3.42).

$$\sigma_a(z) \approx \frac{\varphi_1(z)}{M_1^*} \cdot \sqrt{\frac{\pi f_1 S_{F_1^*}(f_1)}{4(\zeta_{s1} + \zeta_{a1})}} \quad (3.42)$$

Now the peak acceleration can be written as Equation (3.43).

$$\hat{a}(z) = \frac{H}{M_1^*} B_{GR} W_H \left(\frac{z}{H}\right)^\beta \sqrt{\frac{\pi \Phi S_M^*(f_1)}{4(\zeta_{s1} + \zeta_{a1})}} \quad (3.43)$$

### 3.4 Systematic computation steps to calculate across wind ESWL

To simplify the computation procedure involved in evaluating across-wind ESWL and responses, the following sequential steps are outlined

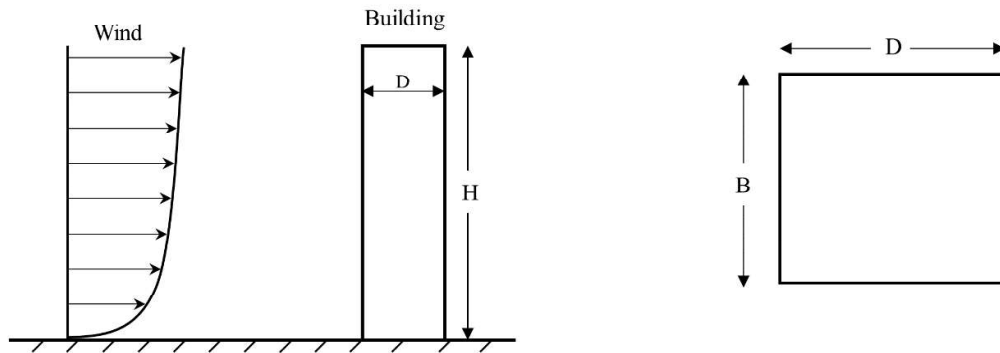
1. Begin by acquiring the pertinent structural and geometric parameters of the building, including height (H), width (B), depth (D), fundamental frequency of the structure ( $f_1$ ), mode shape index ( $\beta$ ), structural damping ratio ( $\zeta_s$ ) and mass per unit height ( $m(z)$ ) at height z. Subsequently, use Equation (3.12) to calculate the first generalized mass denoted as  $M_1^*$ .
2. Proceed to obtain the wind field parameters encompassing mean wind velocity profile exponent ( $\alpha$ ), turbulence intensity of approaching wind ( $I_H$ ) at the top of the considered building, approaching wind pressure at the top of the building ( $W_H$ ), and

mean velocity of approaching wind at the top of the building ( $U_H$ ). Values of wind field parameters are provided in Input Data section (3.6).

3. Determine the background base moment coefficient  $C_{M-B0}$  using Equation (3.36) and the peak factor for the resonant response,  $g_R$  using Equation (3.23). The mode shape index ( $\beta$ ) has been taken as unity, so mode shape correction coefficient ( $\Phi$ ) of generalized aerodynamic force would also become unity.
4. Estimate the reduced base moment power spectral density at first mode frequency,  $S_M^*(n)$  and determine the aerodynamic damping ratio  $\zeta_a$ .
5. Determine the peak across-wind ESWL  $\hat{p}(z)$  with Equations (3.37) using Equations (3.34) and (3.35).
6. Calculate the internal force or other responses along with the induced ESWL.

### 3.5 Methodology

This research investigates a theoretical super high-rise building with 300 m height, located within the city environment. The wind direction and the plan of the building are shown in Figure 3.2. In this study, the systematic computation steps described in Section 3.4 are followed to develop a MATLAB code. The code is dedicated to evaluate the across-wind ESWL and the corresponding responses. The code is provided in Appendix



A. To

**Figure 3.2** Direction of wind and plan of the building

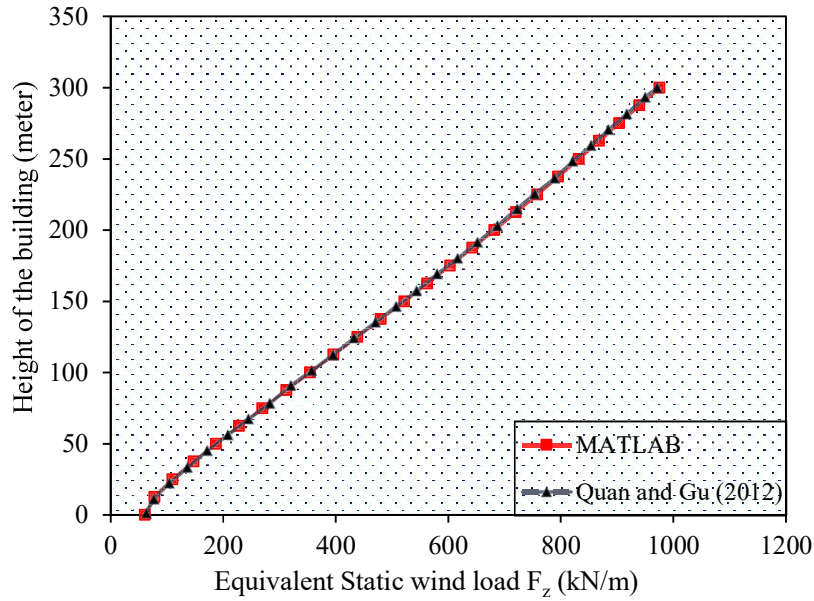


**Figure 3.3** Comparison of Quan and Gu (2012) and MATLAB results

validate the accuracy of the MATLAB code, its results were compared with those obtained by Quan and Gu (2012) and presented in Figure 3.3. Quan and Gu (2012) stated in their assumption number four that the formulation is valid for plan aspect ratio 0.5-2 and height aspect ratio 4-9. To examine the effect of varying the plan aspect ratio (0.5-2), the height aspect ratio is fixed at 4. Similarly, to observe the impact of changing the height aspect ratio (4-9), the plan aspect ratio is kept constant as unity. The upcoming Section 3.6 discusses the values of input parameters used in the computations.

### 3.6 Input data

#### 3.6.1 Structural parameters

The fundamental frequency of all the structures is estimated using IS 875 (Part 3): 2015 and the structural damping ratio is considered as 0.01 (Quan and Gu 2012).

#### 3.6.2 Wind characteristics parameter

Turbulence Intensity of approaching wind at the height of target building is taken as 11%. According to IS 875 (Part 3): 2015, it varies from 7% to 17% for the adopted building

height depending upon the terrain category, the lowest being in open terrain category to the highest in city centres with numerous high-rise structures. The exponent of the mean wind velocity is taken 0.30. A higher value (70 m/s) of basic wind speed has been adopted to see the response of the structure in this range. Design wind pressure at building height is taken as 2996 (kN/m<sup>2</sup>). Mode shape index ( $\beta$ ) is taken as 1.

### 3.6.3 Geometrical parameters

For all the cases height of the building has been fixed as 300 meters (Quan and Gu 2012).

Plan aspect ratio and height aspect ratio have been varied as follows.

#### *Plan aspect ratio*

Plan aspect ratio is the ratio of depth and width of the building. The plan aspect ratio has been varied from 0.5 to 2 keeping the height constant as 300 meters. Table 3.1 shows the dimensions considered. The wind flow is perpendicular to the width B. In Figure 3.4, plan of all the buildings are shown together and buildings are analysed one by one. Plan aspect ratios are taken in the range of 0.5 to 2 with the range of assumptions of Quan and Gu (2012).

**Table 3.1** Details of Plan Aspect Ratio

Plan Aspect ratio (D/B)	Width (B) (meter)	Depth (D) (meter)	Label
0.5	100	50	G
0.75	66.667	50	F
1	50	50	A
1.25	50	62.5	B
1.5	50	75	C
1.75	50	87.5	D
2	50	100	E

**Height aspect ratio**

The height aspect ratio (or simply aspect ratio) is the ratio of the height of the building and the side of the building. In case the side dimensions of the building are different, then the height aspect ratio is the ratio of height of the building and the smaller side of the building. As square buildings are subjected to the maximum along wind and across wind forces, the effect of changing height aspect ratios has been studied for six square in plan buildings. The height aspect ratio is varying from 4 to 9 keeping the plan aspect ratios constant as 1. Table 3.2 shows the dimensions considered for height aspect ratios 4 to 9. Height aspect ratios are considered in the range of 4 to 9 because IS 875 (Part 3): 2015

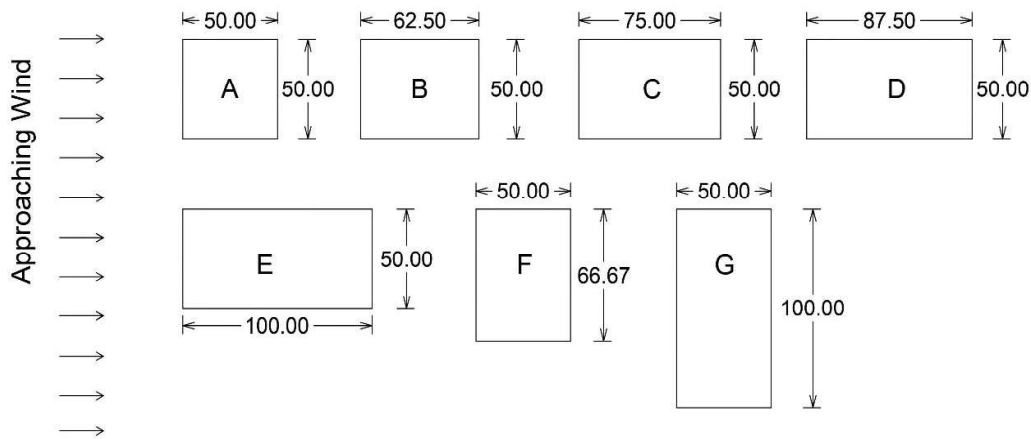


**Figure 3.4** Plan of Buildings considered for study (dimensions are in meter)

recommends using its formulation for buildings with height aspect ratios exceeding 4.

**Table 3.2** Details of height aspect ratio

Height aspect ratio	4	5	6	7	8	9
Side dimension (m)	75	60	50	42.85	37.5	33.33

### 3.7 Results and Discussion

#### 3.7.1 Effect of varying depth on across-wind load and responses

The effect of varying the depth of the building on the ESWL has been studied keeping the width dimension as fixed. Sides parallel to the wind stream are considered as depth of the building (refer plans labelled as A, B, C & D of Figure 3.4). This part of the study

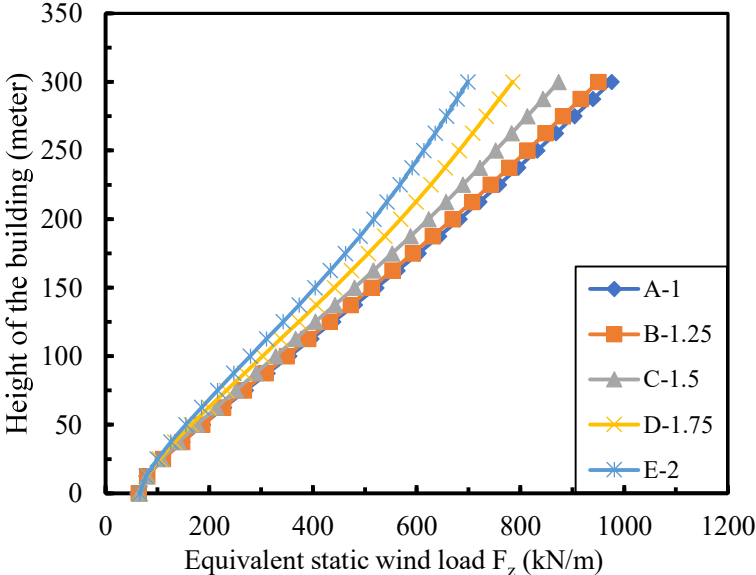


**Figure 3.5 (a)** ESWL along the height of the building for plan aspect ratio 1 to 2

also provides an insight into the effect of varying plan aspect ratios from 1 to 2 on across wind load.

ESWL, shear force, and base bending moment are depicted in Figures 3.5 (a), 3.5 (b), and 3.5 (c) respectively. Building A (square in plan) is exposed to maximum ESWL, shear force and base bending moment compared to the other buildings. For a plan aspect ratio of 1.25, the results are close to the square plan. As the plan aspect ratio increase from 1 to 2, the ESWL, shear force, and base bending moment values decrease. The results of the present study conform to that of Simiu and Scanlan (1996), which states that as the depth of the building increases, the vortex shedding effect on the building decreases, resulting in lesser across wind forces.

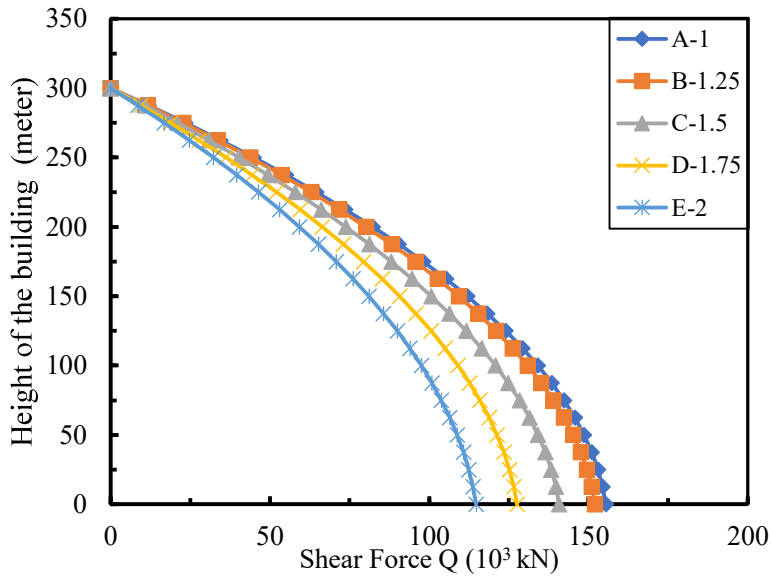


**Figure 3.5 (b)** Shear force along the height of the building for plan aspect ratio 1 to 2

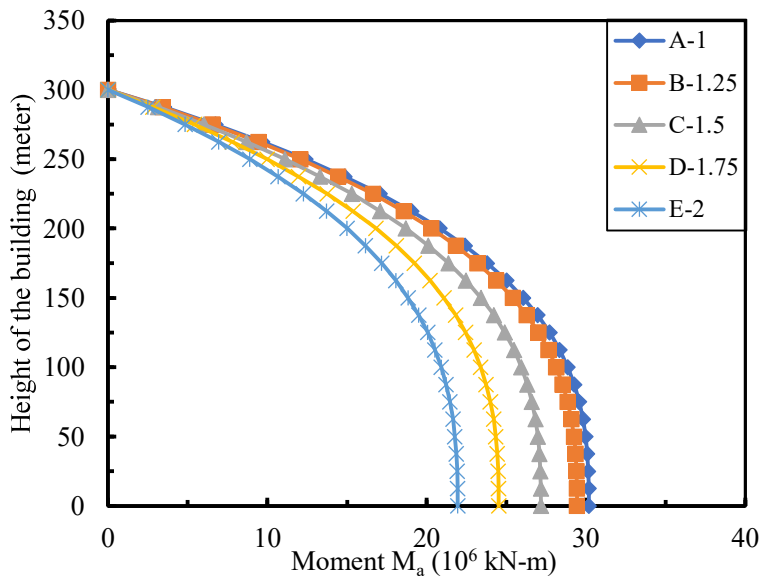


**Figure 3.5 (c)** Bending moment along the height of the building for plan aspect ratio 1 to 2

### 3.7.2 Effect of varying width on across wind load and responses

The effect of varying the width is studied keeping the depth fixed as 50 meters. Sides perpendicular to the wind flow are mentioned as width. The width has been varied as 100 m (case G), 66.67 m (case F), and 50 m (case A). This part of study is carried out to see the effect of the varying the plan aspect ratio from 0.5 to 1 on across wind load.

ESWL, shear force and base bending moment are shown in Figures 3.6 (a), 3.6 (b) and 3.6 (c) correspondingly. Building A (Square in plan) is exposed to maximum ESWL, shear force and base bending moment compared to buildings having plan aspect ratios of 0.75 and 0.5. It can be observed from the figures that as the width of the building is increased the across wind effects are reduced progressively. This is because larger width leads to the higher moment of inertia of the building in across wind direction. Thus, the probability of inducing across wind vibrations becomes substantially lower. The computed values of ESWL, base shear, and base bending moment for across wind cases are listed in Table 3.3 for different plan aspect ratios.

**Table 3.3** Peak values of across wind ESWL, Base Shear and Base bending moment with different plan aspect ratios

Plan aspect ratio	ESWL at the top of the building (kN/m)	Maximum Base Shear due to across wind loading( $10^3$ kN)	Maximum Base Bending Moment due to across wind loading ( $10^6$ kN-m)
0.5	446.6	75.9	14.3
0.75	707.2	116.8	22.3
1	975.7	155.47	30.2
1.25	949.9	152	29.5
1.5	873.5	140.8	27.2
1.75	784.8	127.6	24.5
2	698.7	114.7	21.9

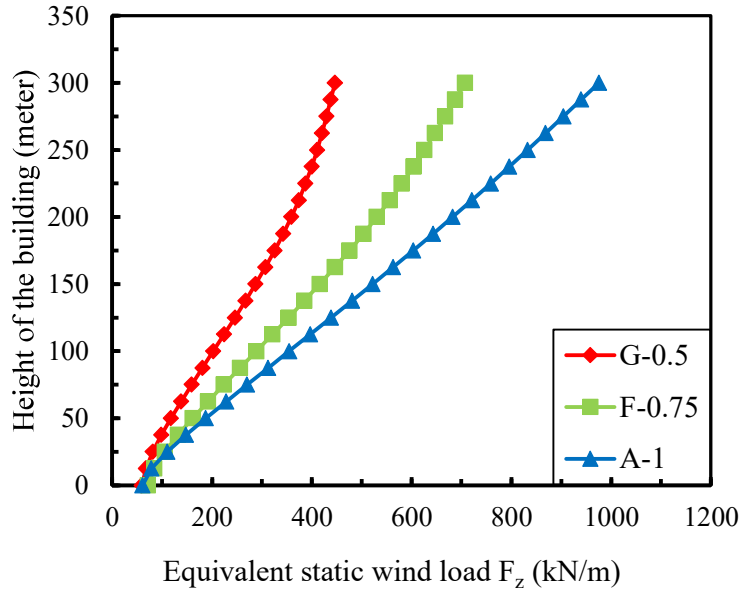


**Figure 3.6 (a)** Across wind ESWL along the height of the building for plan aspect ratio 0.5 to 1

In the range of plan aspect ratios of 0.5 to 2, Table 3.3 clearly shows that the building with plan aspect ratio one (square) has the highest ESWL at the top of the building, followed by the base shear and base bending moment. For a building with a square plan, Hui *et al.* (2017) state that the mean and fluctuating torsion coefficients are significantly higher (1.5 times) than rectangular buildings. The square plan is more vulnerable to across wind force so it must be designed carefully in conjunction with the state of the art mitigation techniques like major modification (*e.g.* tapering, setback, twisting, opening, *etc.*) or minor modification (*e.g.*, corner modifications like rounded, chamfered, recessed corner, *etc.*).

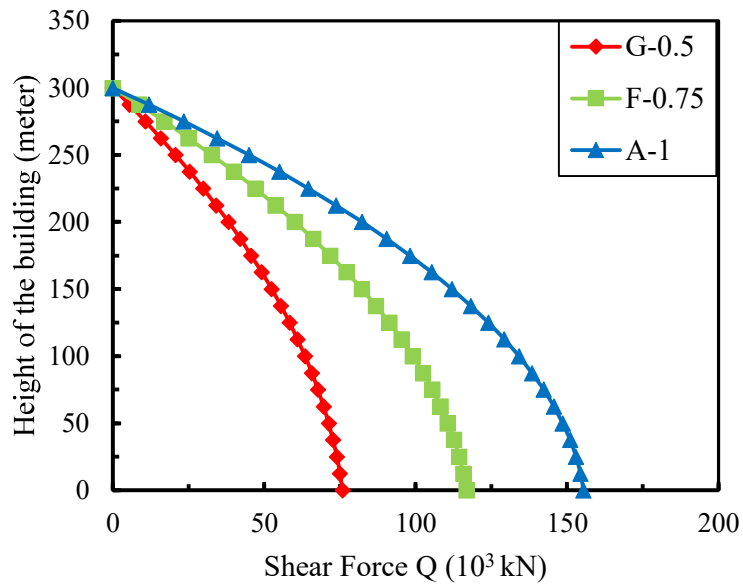


**Figure 3.6 (b)** Shear force along the height of the building for plan aspect ratio 0.5 to 1

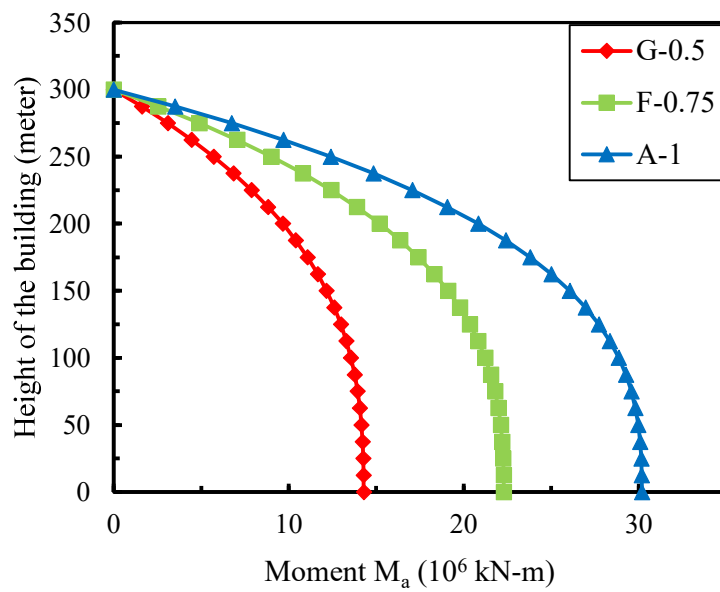


**Figure 3.6 (c)** Bending moment along the height of the building for plan aspect ratio 0.5 to 1

### 3.7.3 Comparison of along & across wind load for various plan aspect ratios

Comparison of estimated along and across wind load is done for plan aspect ratios varying from 0.5 to 2. In Figure 3.7 (a)-(d) and Figure 3.8 (a), it is interesting to note that at the top of the building, across wind load is more than along wind load for plan aspect ratios varying from 1 to 2. However, from Figures 3.8 (b) and 3.7 (c), it is evident that for plan aspect ratios 0.75 and 0.5, along wind ESWL is more than across wind load.

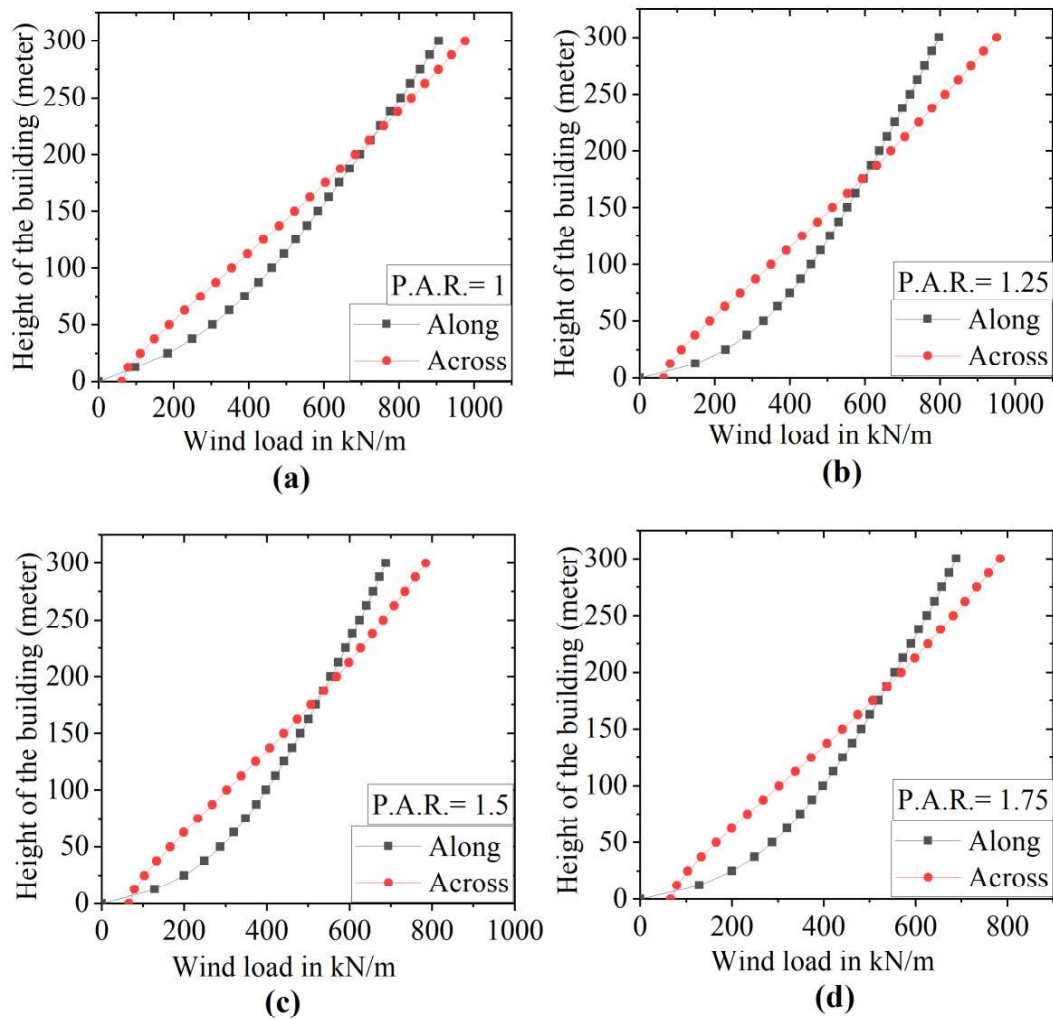


**Figure 3.7** Across and Along wind load for Plan Aspect Ratio (P.A.R.) 1 to 1.75

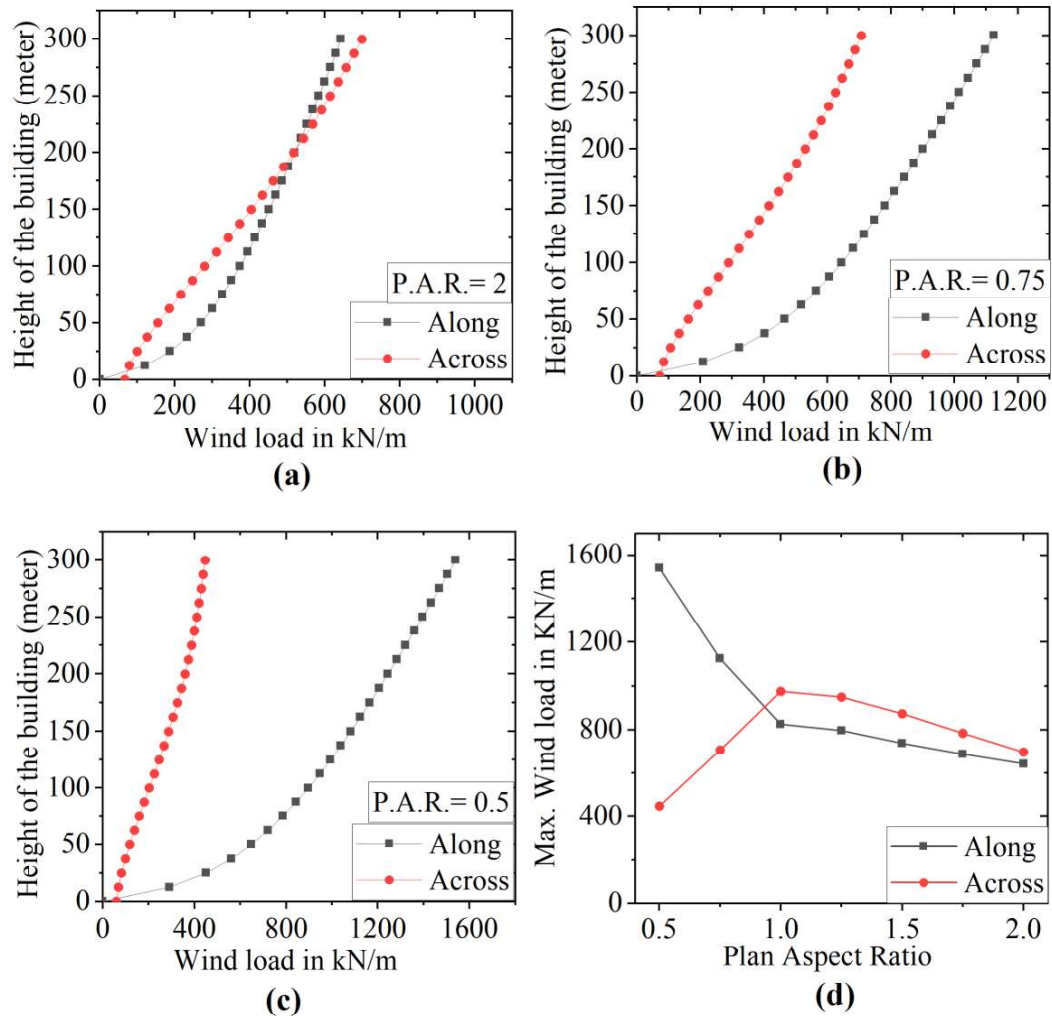


**Figure 3.8** Across wind and Along wind load for Plan Aspect Ratio (P.A.R) (a) 2, (b) 0.75, (c) 0.5 and (d) Along versus Across max. wind load (at the tip of the building)

Figure 3.8 (d) shows the variation of maximum along wind and across wind load for plan aspect ratios varying from 0.5 to 2. Similar to the results of Table 3.3, Figure 3.8 (d) reveals that buildings having a square plan are likely to be subjected to higher across wind loading. Initially plan aspect ratio up to 0.75 the along wind load are comparatively higher than the across wind load. However, buildings with a plan aspect ratio more than one are subjected to higher across wind load than that of along wind load. Ideally, the crossing

point in Figure 3.8 (d) signifies the aspect ratio at which along and across wind load are theoretically identical.

### 3.7.4 Effect of height aspect ratio on across wind load and responses

As observed in previous section, buildings with a square plan are subjected to maximum across wind load. To investigate further, square buildings with different height aspect ratios are analysed in this section. All buildings have the same height of 300 m, while their sides are progressively reduced from 75 m to 33.33 m as shown in Table 3.2.

ESWL, shear force, and base bending moment are shown in Figures 3.9 (a), 3.9 (b), and 3.9 (c). ESWL, shear force and base bending moment increase monotonically as the height aspect ratio increases. ESWL is least for height aspect ratio four and maximum for height aspect ratio nine. The increment in the loads is due to an increment in reduced wind velocity with height aspect ratio. ESWL, shear force, the base bending moment is given in Table 3.4 for different height aspect ratios.

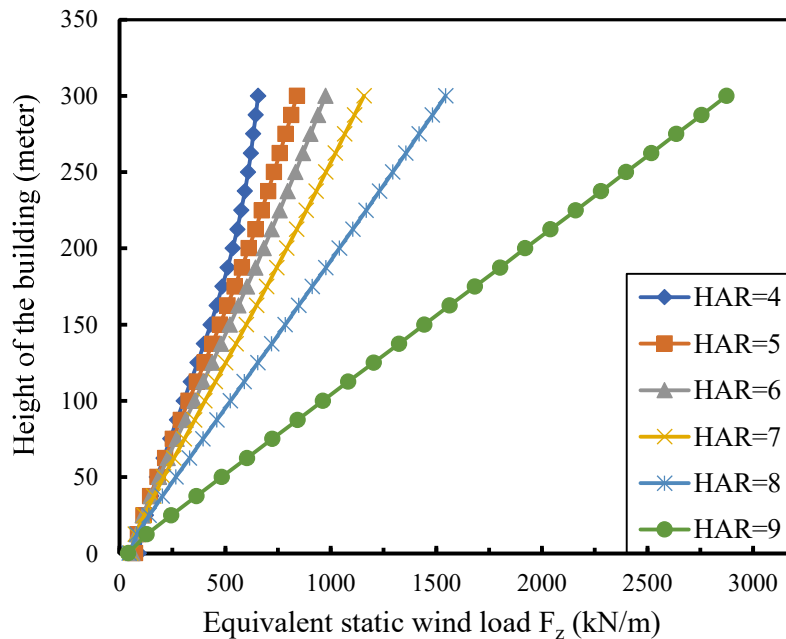


**Figure 3.9 (a)** Across wind ESWL for Height aspect ratios (HAR) 4 to 9

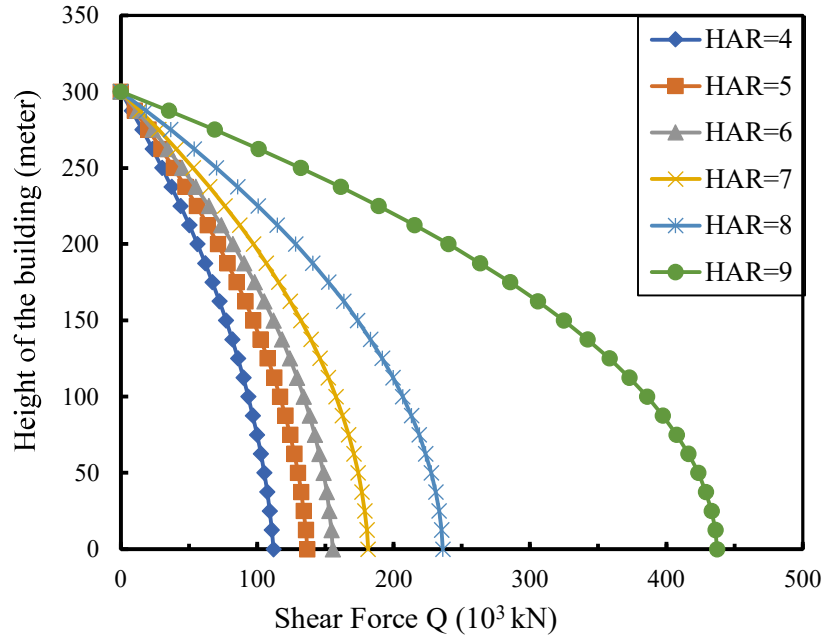


**Figure 3.9 (b)** Shear force along the height of the building for Height aspect ratios (HAR) 4 to 9

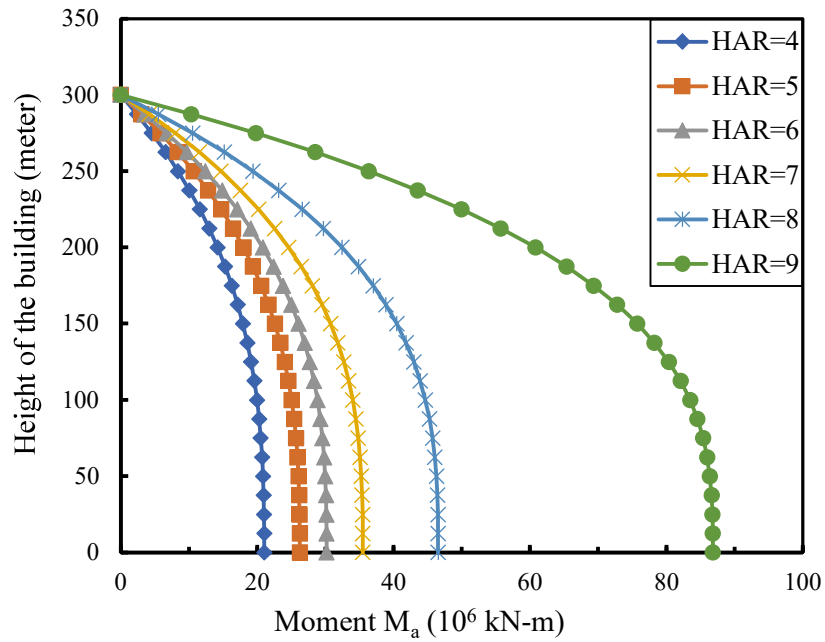


**Figure 3.9 (c)** Bending Moment along the height of the building for Height aspect ratios (HAR) 4 to 9

**Table 3.4** Peak values of across wind ESWL, Base Shear and Base bending moment with different height aspect ratios

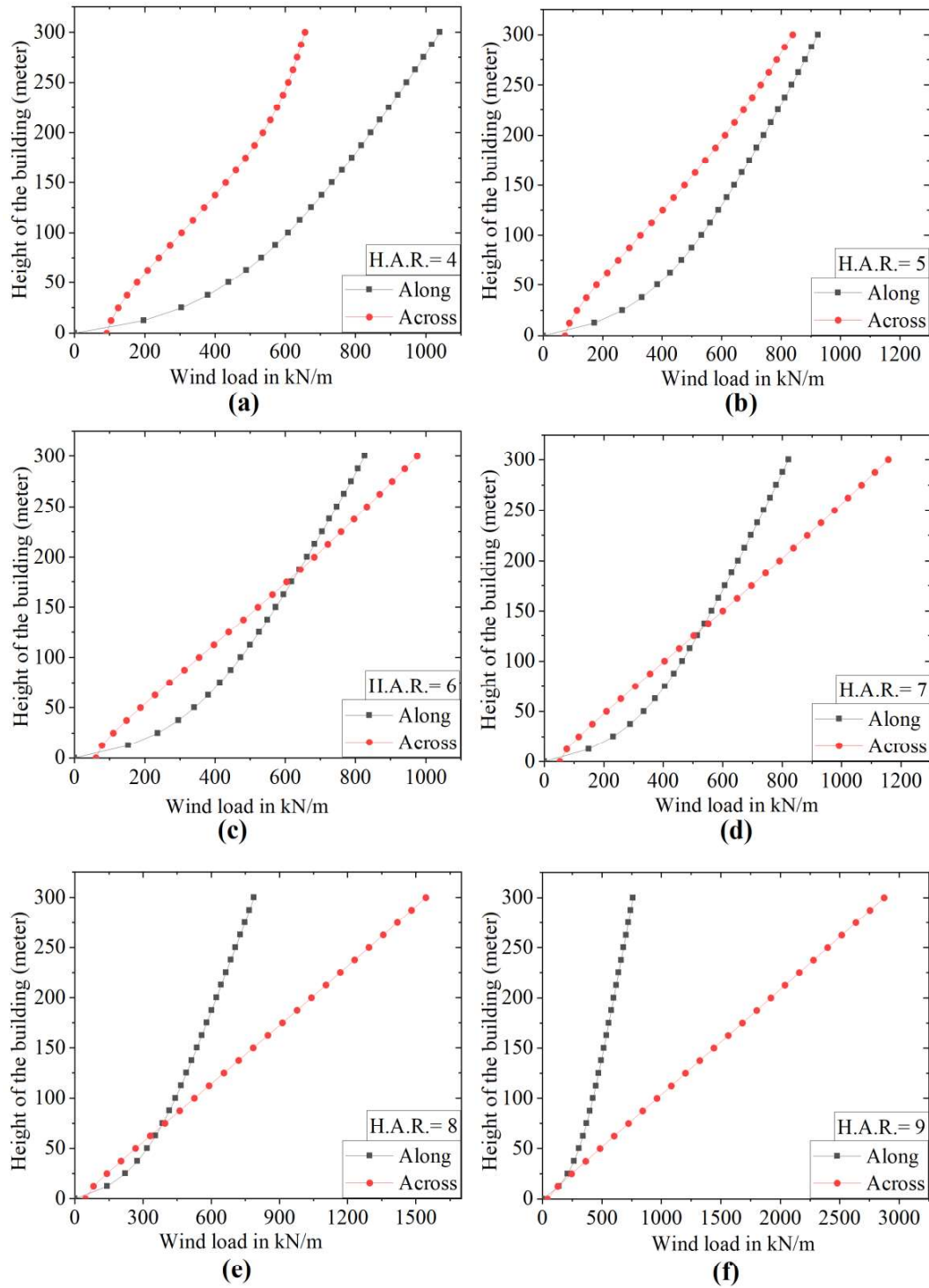
Height aspect ratio	ESWL at the top of the building (kN/m)	Maximum Base Shear due to across wind loading ( $10^3$ kN)	Maximum Base Bending Moment due to across wind loading ( $10^6$ kN-m)
4	656.2	112.1	21.1
5	839.2	136.8	26.3
6	975.7	155.5	30.2
7	1157.2	181.4	35.5
8	1543.9	236.1	46.5
9	2874.3	437.2	86.8

Table 3.4 clearly shows that as the building becomes more slender, all the design forces increase drastically. It is to be noted that buildings with a height aspect ratio beyond 8 should be avoided strictly as the magnitude of across wind ESWL increases drastically beyond height aspect ratio 8. If unavoidable, the buildings should be adequately designed and equipped with additional structural elements.

### 3.7.5 Comparison of along & across ESWL on various height aspect ratios

Comparison of along wind ESWL and across wind ESWL is done for height aspect ratios 4 to 9 keeping plan aspect ratio as 1. This has been done as buildings with square plans experience maximum across wind loading compared to along wind loading. At the top of the building across wind ESWL is more for height aspect ratios 6 to 9 and for height aspect ratios 4 and 5 along wind load is more than across wind load.

As the height aspect ratios are increased, *i.e.*, as the buildings become more slender, both along and across wind response of the structure also increase which is observed from Figure 3.10 (a) to 3.10 (f). However, from height aspect ratios 8 to 9, there is a drastic increase in across wind loading.



**Figure 3.10** Across and Along wind load for Height Aspect Ratio (H.A.R) 4 to 9

The variation of maximum along wind and across wind ESWL affecting the structure for height aspect ratios four to nine is showed in Figure 3.11.

For height aspect ratios 4 and 5 along wind ESWL magnitude is higher compared to across wind ESWL. However, for height aspect ratios 6, 7, 8 & 9, the across wind ESWL magnitude exceeded the along wind ESWL magnitude at height 185m,130m,75m &20m respectively.

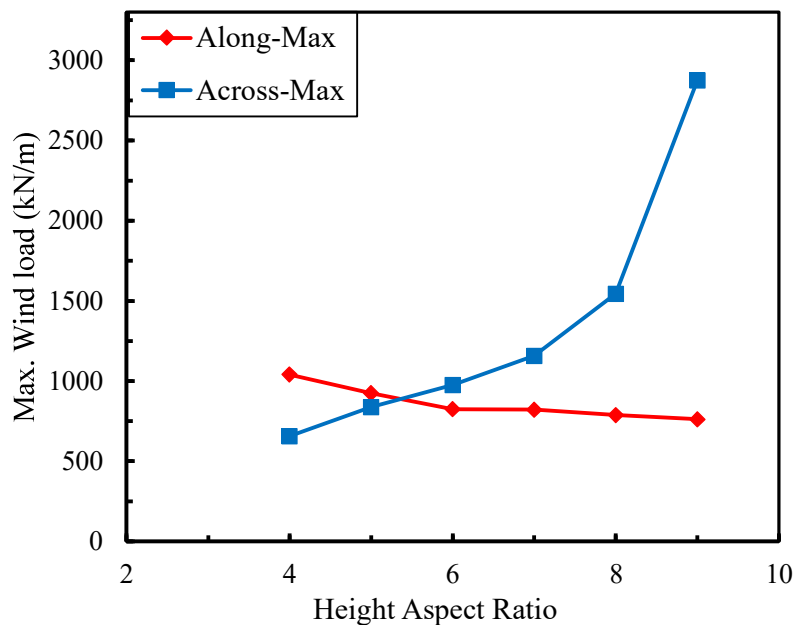


**Figure 3.11** Along *versus* Across max. wind load (at the tip of the building) for height aspect ratio 4 to 9

### 3.8 Concluding remarks

In this chapter, the effect of geometrical parameters on across wind load has been studied. The effect of the plan aspect ratios has been studied in two ways, firstly by varying the depth of the building and secondly by varying the width of the building. Also, the effect of height aspect ratio on the across wind load is studied by changing its plan dimensions keeping the height as constant. As the depth of the building increases, the across wind

load decreases. As the width of the building, *i.e.*, the side perpendicular to the flow increases, the across wind load decreases. Initially, plan aspect ratio up to 0.75, the along wind load are comparatively higher than the across wind load. However, buildings with a plan aspect ratio more than one are subjected to higher across wind ESWL than that of along wind load. In the range of plan aspect ratios from 0.5 to 2, maximum across wind loads are obtained for a building with a plan aspect ratio of one. As the height aspect ratio increases, the across wind load also increases. Beyond height aspect ratio eight, the magnitude of across wind load increases drastically.

Therefore, based on the present study, to build a stronger and safer building against wind loads, it is recommended that designers should avoid buildings square in plan and keep the height aspect ratio below eight.

